NHH

INSTITUTT FOR FORETAKSØKONOMI

DEPARTMENT OF BUSINESS AND MANAGEMENT SCIENCE

FOR 17 2016

ISSN: 1500-4066

November 2016

Discussion paper

The Impact of Bunker Risk Management on CO_2 Emissions in Maritime Transportation Under ECA Regulation

BY

Yewen Gu, Stein W. Wallace AND **Xin Wang**

Norges Handelshøyskole

NORWEGIAN SCHOOL OF ECONOMICS

The Impact of Bunker Risk Management on CO_2 Emissions in Maritime Transportation Under ECA Regulation

Yewen Gu, Stein W. Wallace, Xin Wang

Abstract The shipping industry carries over 90 percent of the world's trade, and is hence a major contributor to CO_2 and other airborne emissions. As a global effort to reduce air pollution from ships, the implementation of the ECA (Emission Control Areas) regulations has given rise to the wide usage of cleaner fuels. This has led to an increased emphasis on the management and risk control of maritime bunker costs for many shipping companies. In this paper, we provide a novel view on the relationship between bunker risk management and CO_2 emissions. In particular, we investigate how different actions taken in bunker risk management, based on different risk aversions and fuel hedging strategies, impact a shipping company's CO_2 emissions. We use a stochastic programming model and perform various comparison tests in a case study based on a major liner company. Our results show that a shipping company's risk attitude on bunker costs have impacts on its CO_2 emissions. We also demonstrate that, by properly designing its hedging strategies, a shipping company can sometimes achieve noticeable CO_2 reduction with little financial sacrifice.

Keywords: Bunker risk management, Maritime bunker management, CO_2 emissions, Stochastic programming, ECA, Fuel hedging, Sailing behavior

Yewen Gu
Department of Business and Management Science, Norwegian School of Economics, Bergen, Norway, e-mail: yewen.gu@nhh.no

Stein W. Wallace
Department of Business and Management Science, Norwegian School of Economics, Bergen, Norway e-mail: stein.wallace@nhh.no

Xin Wang
Department of Industrial Economics and Technology Management, Norwegian University of Science and Technology, Trondheim, Norway e-mail: xin.wang@iot.ntnu.no

1 Introduction

Maritime transport is one of the most important freight transportation modes in the world, since it is by far the most cost effective alternative for transporting large-volume goods between continents. In 2015, more than 90 percent of global trade is carried by sea (ICS, 2015), therefore the shipping industry plays a vital role in the world economy.

Due to the enormous amount of marine fuel consumed by the world fleet, the maritime sector is one of the biggest sources of CO_2 emissions among all transportation industries. International shipping emits approximately 2.2% of the world's anthropogenic CO_2 emissions. This number may further increase to 17% by 2050 if no effective control measure is applied (Cames et al., 2015).

On the other hand, fuel cost is the major cost driver in the shipping industry. It is therefore critical for a shipping company to manage its bunker purchasing and consumption properly. In practice, fuel prices are highly volatile which could bring considerable risks. Bunker risk management is then commonly applied by shipping companies in order to control the risk brought by the high volatility of the fuel cost. For example, risk measures such as CVaR (Conditional Value at Risk) from the field of financial portfolio management may be used to represent a shipping company's risk aversion. Fuel hedging is also one of the popular risk control approaches in the shipping industry. As a contractual tool, it allows the shipping company to reduce its exposure to fuel risk by establishing a fixed or capped cost for its future fuel consumption.

In Gu et al. (2016), a Maritime Bunker Management (MBM) problem that combines tactical fuel hedging and operational ship routing and speed optimization is introduced, which aims to minimize a shipping company's expected total bunker costs based on its risk attitude. Using a case study, the authors show that the integration of the tactical and operational levels of MBM is vital for a shipping company after the implementation of Emission Control Areas (ECA) which regulate sulfur emissions. In this study, the same mathematical model and a similar case are used, but we focus on the impact of a shipping company's bunker risk management on its fleet's CO_2 emissions.

As individual research topics, both CO_2 emissions and bunker risk management have been intensively studied in the maritime transportation literature. Regarding CO_2 emissions, many studies focus on the relationship between speed reduction, also known as slow steaming, and emission reduction. Corbett et al. (2009) evaluate whether speed reduction is a cost-effective option to mitigate CO_2 emissions for ships calling on US ports. Cariou (2011) examines the break-even price of the maritime bunker at which the slow steaming strategy and the corresponding CO_2 emissions reduction are sustainable in the long run. Lindstad et al. (2011) investigate the impacts of slow steaming on CO_2 emissions and costs in maritime transport. They show that the emissions of CO_2 can be decreased by 19% with a negative abatement cost and by 28% at a zero abatement cost if a proper slow steaming strategy is applied. Maloni et al. (2013) show that under current conditions, extra slow steaming can achieve substantial reductions in both total cost and CO_2 emissions.

Tai and Lin (2013) compare the unit CO_2 emissions in the cases when daily frequency or slow steaming strategies is applied in international container shipping on Far East-Europe routes. Wong et al. (2015) generalize the traditional discrete cost-based decision support model in slow steaming maritime operations into novel continuous utility-based models which balance fuel consumption, carbon emission and service quality. Another research direction on CO_2 reduction in maritime transportation is green ship routing and scheduling. It extends the traditional ship routing and scheduling problems and integrates environmental concerns. Related studies can be found in, for instance, Qi and Song (2012), Kontovas (2014) and De et al. (2016).

As regards bunker risk management, fuel hedging is the most commonly used instrument in maritime transportation. Menachof and Dicer (2001) argue that the bunker surcharges widely applied in liner shipping can be eliminated and replaced by the utilization of oil commodity futures contracts. The hedging effectiveness of futures contracts among different fuel commodities is examined and compared in Alizadeh et al. (2004). Wang and Teo (2013) offer a comprehensive review of all the fuel hedging instruments available on the market and integrate fuel hedging into the modeling of liner network planning. Pedrielli et al. (2015) propose a game theory based approach to optimize the fuel hedging contract so that the expected profit for the bunker supplier and the expected refueling cost for the shipping company are maximized and minimized, respectively.

To the best of our knowledge, none of the studies in the literature has explored the relationship between bunker risk management and CO_2 emissions in maritime transportation. Such a gap in knowledge is, to a certain degree, expected as the former had no impact on the latter in the past. This is because in most circumstances, the sailing pattern of the fleet (and hence its CO_2 emissions) is relatively fixed and irrelevant to the shipping company's bunker risk management, i.e., the shortest path and the slowest possible speed is usually chosen during the whole voyage, no matter what actions are taken in terms of the company's bunker risk management, such as the amounts of marine fuel hedged.

However, things have changed significantly in the shipping industry during the last decade due to the implementation of the ECA regulation. It is a regional sulfur emission control regulation that restricts the maximum sulfur content in the marine bunker burnt inside the regulated areas, see Fig. 1. The ECA regulation has forced the shipping companies, who has not invested in sulfur emission reduction technologies (scrubber system or liquefied natural gas powered propulsion), to switch their fuels from the traditional heavy fuel oil (HFO) to the expensive marine gasoline oil (MGO) when their vessels navigate inside ECA.

One of the consequences of the ECA regulation and the substantial price difference between MGO and HFO is that the shipping companies no longer necessarily operate their fleet in the old-fashioned "shortest and slowest possible" way. They now have the motivation to change the sailing behavior of the vessels, so as to minimize the total bunker cost and simultaneously comply with the ECA regulation. Two types of potential change in sailing behavior, namely speed differentiation and ECA-evasion, are shown in Doudnikoff and Lacoste (2014) and Fagerholt et al. (2015).

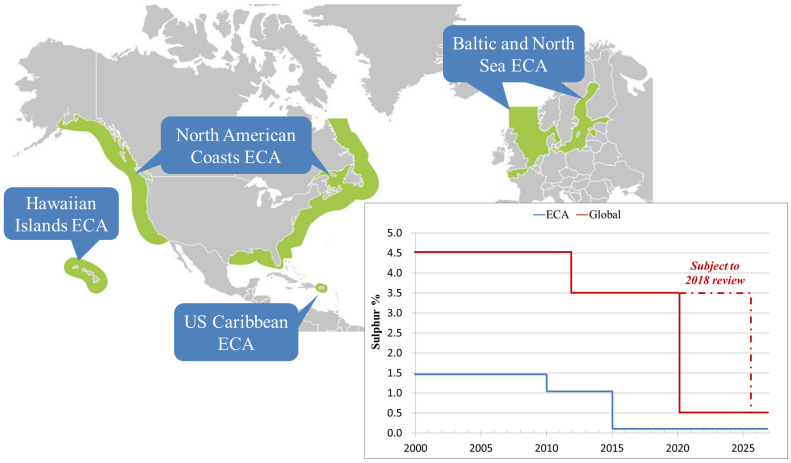

Fig. 1: Map and requirements of the Emission Control Areas.

We illustrate these two types of sailing behavior change in Fig. 2. First, in order to reduce the consumption of MGO, a ship may choose to use different speeds inside and outside ECA, as shown in Fig. 2a, if the voyage involves both regulated and unregulated sea areas. Second, a vessel may make a detour so that the sailing distance inside ECA, and hence its MGO consumption, can be considerably decreased, see for example Fig. 2b. However, to what extent the speed differentiation and ECA-evasion strategies will be applied depends on the price difference between MGO and HFO. For example, if the price difference increases, so will the incentive to reduce MGO consumption, in which case sailing a route with lower ECA involvement may be more beneficial.

A vessel's CO_2 emissions mainly depend on its fuel consumption. The CO_2 emission factors we use in this paper for MGO and HFO are 3.082 (tonnes/tonne fuel) and 3.021 (tonnes/tonne fuel), respectively (Psaraftis and Kontovas, 2009). Therefore, it is the total amount of the two fuels consumed that affects the CO_2 emissions the most, rather than the different combination of the two. Fuel consumption is further determined by the vessel's sailing speed and traveling distance. After the introduction of ECA, the shipping company's optimal speed and routing choices, which may include speed differentiation and ECA evasion, also depend on the prices of the two fuels and the associated hedging decisions made (Gu et al., 2016). In this paper, we seek to investigate how different actions taken in bunker risk management, including different settings of risk aversion and fuel hedging strategies, impact the shipping company's optimal speed and routing choices and the corresponding CO_2 emissions.

We use the stochastic programming model introduced in Gu et al. (2016), and propose various comparison tests based on different levels of risk aversion, fuel hedging strategies and fuel prices. The tests are performed on a case based on a real liner service offered by Wallenius Wilhelmsen Logistics (WWL), one of the

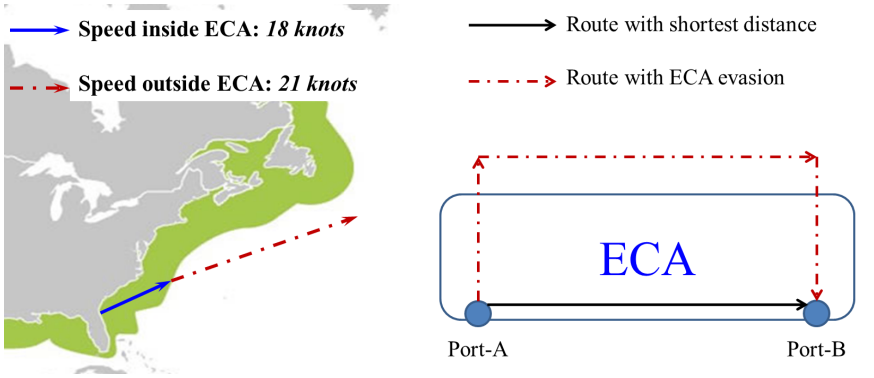

(a) Speed differentiation (b) ECA-evasion

Fig. 2: Two types of sailing behavior change after the implementation of ECA regulation.

world's largest liner service providers for rolling equipment. We aim to provide a novel view on the relationship between bunker risk management and CO_2 emissions, which would hopefully contribute to the worldwide effort in reducing greenhouse gas emissions.

The rest of the paper is structured as follows. Section 2 gives the description of the Maritime Bunker Management (MBM) problem and the mathematical model. In Sect. 3 we introduce the test case and the scenario generation process. Section 4 presents the results of our computational study. Our conclusion is given in Sect. 5.

2 The problem and mathematical model

The problem description and the mathematical formulation are given in this section. In Sect. 2.1, we summarize the settings and assumptions of the problem. The mathematical formulation is then presented in Sect. 2.2.

2.1 Problem statement

First, we introduce four important terms, *loop*, *leg*, *leg option* and *stretch*, which are frequently used in this paper, see Fig. 3 for illustration. A *loop* refers to a round trip calling several ports in a predetermined order, while a *leg* refers to the voyage between two consecutive ports in the loop. A *leg option* represents a possible sailing path for a leg. For different leg options of a same leg, the total sailing distance and the sailing distance inside ECA are also different. A leg option may have one or

more *stretches*. When the vessel crosses the ECA border, the current stretch ends and a new one begins. We also combine the stretches of the same type (on which we assume the same speed) for every single leg option, and thus represent each leg option with only two segments: the ECA stretch and the non-ECA stretch. For example, in Fig. 3c, we combine Stretch 1 and Stretch 3 as the ECA stretch.

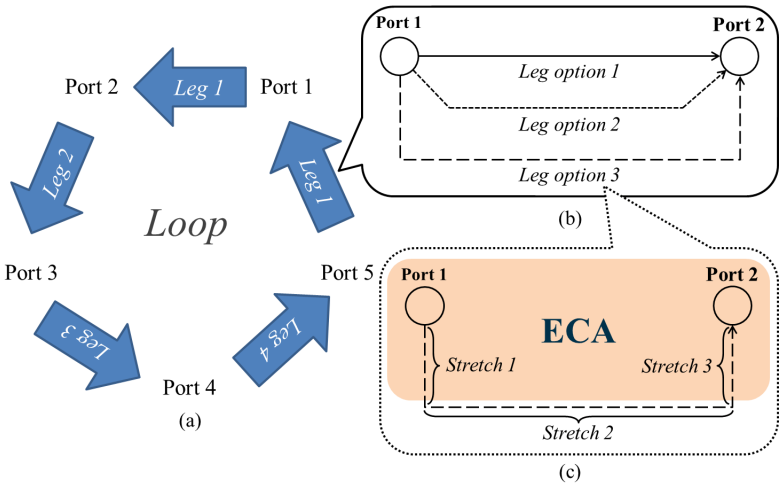

Fig. 3: Illustration of a loop, and its associated legs, leg options and stretches.

For simplification, the MBM problem in this paper only considers one single vessel operating on one single loop. The length of the planning period is assumed to be equal to the scheduled time for the vessel to finish a round trip on the loop. The sequence of the port calls on the loop and the related leg information, including all possible leg options for every leg and the associated stretches, are also assumed to be given as input to our model.

As an essential instrument in bunker risk management, fuel hedging reduces the fuel consumers' exposure to financial risk caused by volatile fuel prices. We consider the so called *forward-fuel contract with exit terms and physical supply* (FFC in the following) in this study. An FFC endows the shipping company with the right to buy a specified amount of a certain type of fuel with a predetermined price during an agreed time period. The forward price of a certain fuel in the FFC is normally higher than this fuel's expected price during the contract period. We assume this to be the case in our tests as well, and as a result, a risk-averse shipping company can, and normally will, use FFC for risk control purposes, while a risk-neutral one never enters the forward market due to the expected loss. However, if the shipping realizes that the remaining fuel in the ongoing FFC is no longer needed and decides to terminate the contract, the leftovers are sold back to the fuel supplier with a penalty.

The spot prices for MGO and HFO fuels during the planning period are assumed to be stochastic, and the MBM problem can be described using a two-stage model

with scenarios representing the stochastics. In the first stage, decisions with respect to the amounts of MGO and HFO to be hedged in an FFC must be made at the beginning of the planning period. The spot prices of the two fuels in different scenarios are then realized in the second stage and are assumed to remain constant during the whole planning period. Several operational decisions will be made afterwards based on the realized fuel prices and the first-stage hedging decisions. These second-stage decisions are made of two major parts. The first consists of speed and routing choices on each leg. The second part consists of fuel allocation decisions, i.e. how much spot- and forward-fuels should be used during operations. The objective of the MBM problem is to minimize the total bunker cost which is the sum of the first-stage purchasing costs of the forward fuels and the expected second-stage costs on spot fuels and penalties for unused forward fuels, meanwhile control the bunker cost risk within a desirable level.

The relationship between a vessel's sailing speed and its fuel consumption per unit distance is normally considered as a quadratic function (Norstad et al., 2011). We use a piecewise linearisation approach (Andersson et al., 2015) to approximate the fuel consumption rate for different sailing speeds, as shown in Fig. 4. Note that an overestimation is expected in the application of this approach (see Andersson et al. for detailed discussion), but it is normally insignificant as long as sufficient discrete speed points are used. A good estimation of the relation between speed and traveling time can also be made using this approach.

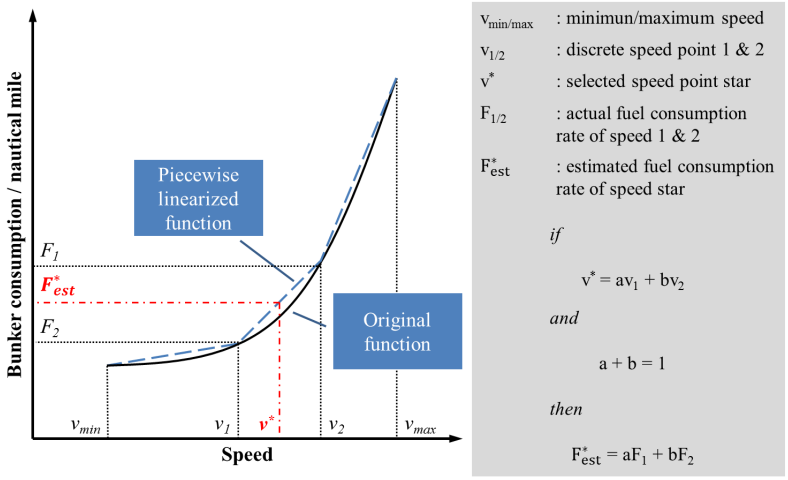

Fig. 4: Piecewise linearisation of the fuel consumption function.

As part of the risk control measures for bunker risk management, we model the risk attitude of the shipping company using a Conditional Value-at-Risk (CVaR) approach, which is extensively used in the field of financial risk management to evaluate various risks. In our model, we impose CVaR constraints on the expected

total bunker costs to achieve the desired risk control effect. Two key parameters, a confidence level and a maximum tolerable CVaR value, are defined and used as inputs for our model. For instance, if the confidence level and the maximum CVaR value are set to 95% and 1.2 million USD, respectively, the CVaR constraints will then ensure that the expected total bunker costs in the worst 5% cases will not exceed 1.2 million USD during the planning period.

2.2 Mathematical formulation

The mathematical formulation is presented as follows:

Sets

J	Set of sailing legs along the loop
R_j	Set of leg options for Leg j
V	Set of feasible discrete speed points for the ship
S	Set of scenarios

Parameters

P^{MGO-F}	Price per ton of MGO agreed in the forward-fuel contract
P^{HFO-F}	Price per ton of HFO agreed in the forward-fuel contract
P_s^{MGO-S}	Price per ton of MGO on spot market under Scenario s
P_s^{HFO-S}	Price per ton of HFO on spot market under Scenario s
P^{MGO-P}	Penalty per ton for the unused MGO left in the forward-fuel contract
P^{HFO-P}	Penalty per ton for the unused HFO left in the forward-fuel contract
$\overline{W}_j$	Latest starting time for Leg j
W_j^S	Service time for Leg j in the departing port
W_{jrv}^{ECA}	Sailing time on ECA stretches on Leg j under Leg option r with Speed v
W_{jrv}^{N}	Sailing time on non-ECA stretches on Leg j under Leg option r with Speed v
D_{jr}^{ECA}	Sailing distance on ECA stretches on Leg j under Leg option r
D_{jr}^{N}	Sailing distance on non-ECA stretches on Leg j under Leg option r
F_v	Fuel consumption per unit distance sailed with speed alternative v (same for both HFO and MGO)
p_s	Probability of scenario s taking place
γ	Confidence level applied in CVaR
A_γ	The maximum tolerable CVaR value under confidence level γ

Decision variables

x_{jrvs}^{ECA}	Weight of speed choice v used on ECA stretches on Leg j with Leg option r under scenario s

x^N_{jrvs}	Weight of speed choice v used on non-ECA stretches on Leg j with Leg option r under scenario s
y_{jrs}	Binary variables representing the decisions on route selection, equal to 1 if Leg option r is sailed on Leg j under scenario s, and 0 otherwise
z^{MGO-S}_{js}	Amount of MGO from spot market used on Leg j under scenario s
z^{MGO-F}_{js}	Amount of MGO from forward contract used on Leg j under scenario s
z^{HFO-S}_{js}	Amount of HFO from spot market used on Leg j under scenario s
z^{HFO-F}_{js}	Amount of HFO from forward contract used on Leg j under scenario s
u^{MGO-F}_{s}	Amount of unused forward MGO left at the end of the planning period under scenario s
u^{HFO-F}_{s}	Amount of unused forward HFO left at the end of the planning period under scenario s
m^{MGO-F}	Agreed amount of MGO in the forward contract
m^{HFO-F}	Agreed amount of HFO in the forward contract
α	Artificial variable for CVaR constraints
h_s	Artificial variables for CVaR constraints under scenario s

The mathematical formulation of the model starts here:

$$\begin{aligned}\min \quad & P^{MGO-F}m^{MGO-F} + P^{HFO-F}m^{HFO-F} \\ & + \sum_{s\in S} p_s \Bigg\{ \sum_{j\in J} \left(P^{MGO-S}_s z^{MGO-S}_{js} + P^{HFO-S}_s z^{HFO-S}_{js} \right) \\ & - (P^{MGO-F} - P^{MGO-P}) u^{MGO-F}_s - (P^{HFO-F} - P^{HFO-P}) u^{HFO-F}_s \Bigg\}\end{aligned} \tag{1}$$

Subject to

$$\overline{W}_{j+1} \geq \overline{W}_j + W^S_j + \sum_{r\in R_j} \sum_{v\in V} \left(W^{ECA}_{jrv} x^{ECA}_{jrvs} + W^N_{jrv} x^N_{jrvs} \right) \qquad s \in S, j \in J \tag{2}$$

$$\sum_{v\in V} x^{ECA}_{jrvs} = y_{jrs} \qquad s \in S, j \in J, r \in R_j \tag{3}$$

$$\sum_{v\in V} x^{N}_{jrvs} = y_{jrs} \qquad s \in S, j \in J, r \in R_j \tag{4}$$

$$\sum_{r\in R_j} y_{jrs} = 1 \qquad s \in S, j \in J \tag{5}$$

$$z^{MGO-F}_{js} + z^{MGO-S}_{js} = \sum_{r\in R_j} \sum_{v\in V} F_v D^{ECA}_{jr} x^{ECA}_{jrvs} \qquad s \in S, j \in J \tag{6}$$

$$z^{HFO-F}_{js} + z^{HFO-S}_{js} = \sum_{r\in R_j} \sum_{v\in V} F_v D^{N}_{jr} x^{N}_{jrvs} \qquad s \in S, j \in J \tag{7}$$

$$\sum_{j\in J} z_{js}^{MGO-F} + u_s^{MGO-F} = m^{MGO-F} \qquad s \in S \tag{8}$$

$$\sum_{j\in J} z_{js}^{HFO-F} + u_s^{HFO-F} = m^{HFO-F} \qquad s \in S \tag{9}$$

$$y_{jrs} \in \{0,1\} \qquad s \in S, j \in J, r \in R_j \tag{10}$$

$$x_{jrvs}^{ECA}, x_{jrvs}^{N} \geq 0 \qquad s \in S, j \in J, r \in R_j, v \in V \tag{11}$$

$$z_{js}^{MGO-F}, z_{js}^{MGO-S}, z_{js}^{HFO-F}, z_{js}^{HFO-S} \geq 0 \qquad s \in S, j \in J \tag{12}$$

$$u_s^{MGO-F}, u_s^{HFO-F} \geq 0 \qquad s \in S \tag{13}$$

CVaR constraints:

$$\alpha + \frac{1}{1-\gamma} \sum_{s\in S} p_s h_s \leq A_\gamma \tag{14}$$

$$h_s \geq 0 \qquad s \in S \tag{15}$$

$$\begin{aligned} h_s \geq\ & P^{MGO-F} m^{MGO-F} + P^{HFO-F} m^{HFO-F} \\ & - (P^{MGO-F} - P^{MGO-P}) u_s^{MGO-F} - (P^{HFO-F} - P^{HFO-P}) u_s^{HFO-F} \\ & + \sum_{j\in J} \left(P_s^{MGO-S} z_{js}^{MGO-S} + P_s^{HFO-S} z_{js}^{HFO-S} \right) - \alpha \qquad s \in S \end{aligned} \tag{16}$$

The objective function (1) minimizes the expected total bunker cost for the planning period. The purchasing costs for the stated amounts of both fuels in the FFC are given in the first line of Eq. 1. The second line of the objective function refers to the expected costs for the consumption of spot-fuels. The last line represents the treatment of the unused forward-fuels. At the end of the planning period, the leftovers in the FFC (if any) are sold back to the bunker supplier at "buyback" prices, computed as their contractual forward prices subtracted by a penalty.

Constraints (2) enforce the time constraints for all sailing legs according to the schedule. Constraints (3) and (4) connect x- and y-variables with respect to the speed-routing choices in ECA and non-ECA stretches, respectively. They ensure that the sums of the speed weights, x_{jrvs}^{ECA} and x_{jrvs}^{N} respectively for ECA and non-ECA stretches, are equal to 1 if Leg option r is chosen for Leg j in Scenario s, and 0 otherwise. Constraints (5) ensure that only one leg option is used on any specific leg. Constraints (6) and (7) make sure that for each scenario the sum of the spot- and forward-fuels used on each leg equals the actual fuel consumption on that leg based on the speeds and leg options chosen. Constraints (8) and (9)

ensure that the forward-fuels used plus the leftovers equal the agreed amounts in the forward contract. Constraints (10) - (13) define the domains of the decision variables. Constraints (14) - (16) are the CVaR constraints representing the risk attitude of the shipping company, restricting the risk on the total bunker costs to be within an acceptable level.

It is important to notice that the CO_2 emissions are not directly considered in the formulation. Instead, they can be calculated based on the optimal solutions obtained using the CO_2 emission factors for the two fuels (see Sect. 1), 3.082 (tonnes/tonne fuel) and 3.021 (tonnes/tonne fuel) for MGO and HFO, respectively. More details will be discussed in Sect. 4.1.

3 The test case and scenario generation

In this section, we briefly describe the test case in Sect. 3.1, while the scenario generation process is discussed in Sect. 3.2.

3.1 The test case

The case considered in this paper is based on a liner service offered by Wallenius Wilhelmsen Logistics (WWL). The company offers roll-on roll-off (RoRo) services for transporting cars, trucks and other types of rolling equipment. In our case, the service loop and its corresponding schedule are adapted from one of WWL's Europe-Americas trade lanes. The sequence of the port calls in the loop is shown in Table 1. The scheduled total traveling time for a round trip on this loop is 35 days. We therefore also set the planning period to 35 days.

Table 1: Sequence of the port calls in the case loop

	Origin Port	Destination Port
Leg 1	Brunswick	Galveston
Leg 2	Galveston	Charleston
Leg 3	Charleston	New York
Leg 4	New York	Bremerhaven
Leg 5	Bremerhaven	Brunswick

We further assign five leg options to each leg in the case loop. Although different leg options of a specific leg share the same origin and destination ports, they differ in terms of ECA, non-ECA and total sailing distances. As an example, Fig. 5 illustrates all five leg options of Leg 3 (Charleston-New York), where Leg option 1 takes the shortest possible path which is completely inside ECA, and Leg option 5, on the

contrary, has the least ECA sailing. The detailed information about sailing distances for each leg option of every leg is displayed in Table 2.

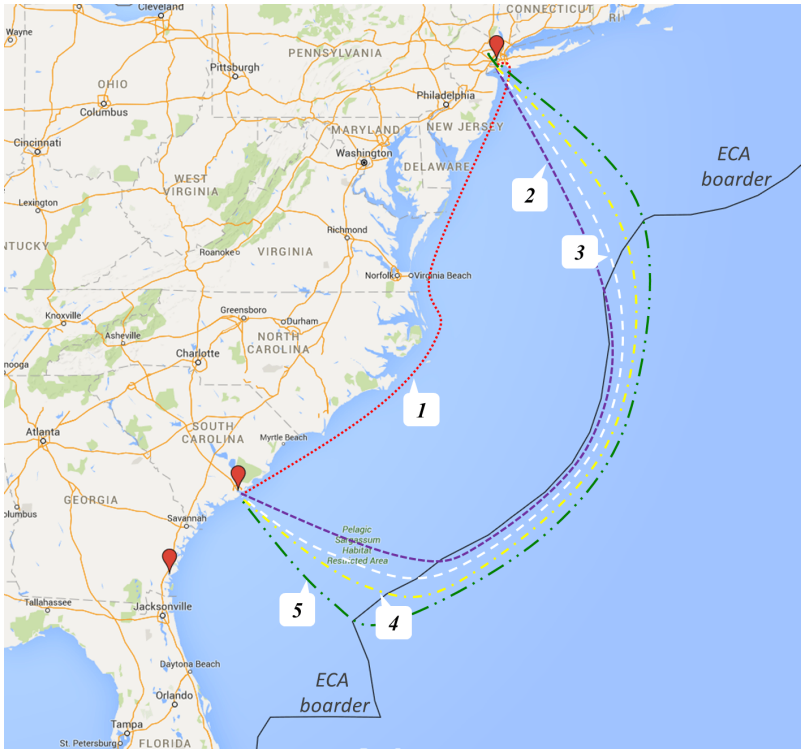

Fig. 5: Five leg options for Leg 3 (Charleston - New York). (Google Maps, 2016)

Table 2: Travelling distances for all ECA/non-ECA stretches

Nautical mile ECA / *non-ECA*	Option 1	Option 2	Option 3	Option 4	Option 5
Leg 1	1191 / 35	569 / 774	495 / 870	469 / 905	408 / 1062
Leg 2	1271 / 34	686 / 704	524 / 906	458 / 1083	397 / 1241
Leg 3	632 / 0	560 / 330	499 / 429	443 / 515	423 / 602
Leg 4	1767 / 1629	1379 / 2125	1042 / 2503	899 / 2652	752 / 2903
Leg 5	2393 / 1626	1110 / 2984	1013 / 3109	817 / 3337	751 / 3428

Additionally, the fuel consumption data we use is collected from the historical record of a real RoRo ship under normal conditions. Fig. 6 shows the fuel consump-

tion per nautical mile for seven selected discrete speed points ranging from 15 to 24 knots.

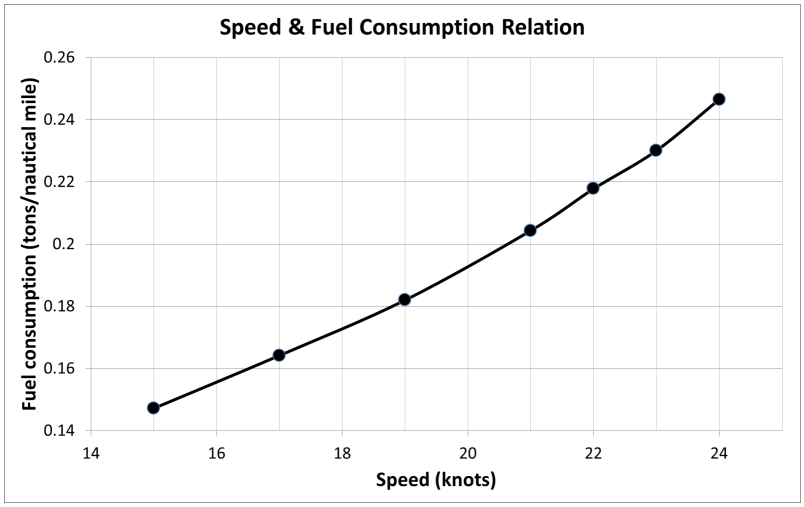

Fig. 6: Speed and fuel consumption relation for the selected discrete speed points

3.2 Scenario generation

As mentioned earlier, the uncertainties considered in our problem refer to the spot prices for MGO and HFO. We assume we know their marginal distributions and the correlation between them, and apply a version of the scenario-generating heuristic developed by Høyland et al. (2003) in order to generate scenarios for fuel prices. However, since fuel prices are significantly dependent over time, generating fuel prices using distributions derived from historical data directly can be problematic. For example, the generated fuel prices will not be representative if the historical data during the past booming period (e.g. 2008) is directly used in the process of scenario generation, when the current market is actually in recession.

Therefore, we use a two-step approach to construct the scenarios for the spot-fuel prices for the next planning period. As a first step, we observe the latest fuel prices on the spot market and use them as base prices, which are also the *expected* spot prices during the planning period. Then, we generate *price increments* using the scenario generation heuristic, either positive or negative, and add them to the base prices. This approach corresponds to the special dynamic of the development of fuel price, which can be seen as a Lévy process with independent increments (Krichene, 2008; Gencer and Unal, 2012).

We use the historical data provided by Clarkson Research Services Limited (Clarkson, 2015) to obtain an estimation of the distributions and correlation for the price increments. The data is collected from three major ports, Rotterdam, Houston and Singapore, and consists of monthly prices of the two fuels (HFO and MGO) at these ports from January 2000 to December 2015. According to the data, the price increments of HFO and MGO are positively correlated and the correlation coefficient is estimated at 0.75. Furthermore, we assume triangular distributions for the random increments. The lower limit, mode and upper limit that control the marginal distributions applied in the scenario-generating heuristic are set to (-40, 0, 40) and (-120, 0, 120) for HFO and MGO, respectively. The latest observations of the spot-fuel prices (used as base prices, or expected spot prices) are from December 2015, and the prices of HFO and MGO are 150 USD/tonne and 375 USD/tonne, respectively. Also note that in our model the forward prices are always set to be marginally higher than the corresponding expected spot prices to prevent speculation.

Finally, an in-sample stability test (Kaut and Wallace, 2007) is performed to check the reliability of the scenario generation process. By comparing the results with different scenario trees generated under the same conditions, this test checks whether the optimal objective function value has a significant dependence on the specific scenario tree used. In our case, 10 scenario trees, each with 100 scenarios, are generated. The difference among the objective values solved with all 10 scenario trees is smaller than 0.02%, which shows that the scenario generation process used in this paper is stable and reliable.

4 Computational study

In this section, we investigate how CO_2 emissions may be affected by a shipping company's risk attitude (Sect. 4.1), and its fuel hedging decisions (Sect. 4.2).

4.1 Impact of risk attitude on CO_2 emissions

In our model, the shipping company's risk attitude towards its total bunker costs, i.e. its risk aversion level, can be represented by a maximum tolerable CVaR value (A_γ) and a confidence level (γ, set to a fixed value of 95% in our study). The $A_{95\%}$ value determines an upper bound of the average total cost allowed in the worst (5%) cases. A larger $A_{95\%}$ then corresponds to a higher tolerance of extreme risk, and hence a lower risk aversion level. This allows us to use different $A_{95\%}$ values to represent the different levels of risk aversion, in order to study the impact of the company's risk attitude on its CO_2 emissions.

4.1.1 Effect of changing risk aversion levels

First, we assume a "standard" risk aversion level for our case study. The corresponding $A_{95\%}$ is set to 390,000 USD which is approximately 1%[1] higher than the optimal total bunker cost in a risk-neutral case, or the objective function value obtained when solving the problem without the CVaR constraints. The standard risk aversion level is then used as a benchmark for comparing the CO_2 emissions at different risk aversion levels.

We use in total 8 different $A_{95\%}$ values, ranging from 388,000 USD (extremely risk-averse) to 400,000 USD (least risk-averse). We also test the risk-neutral case which can be equivalently considered as having an enormously large $A_{95\%}$ value and the CVaR constraints are thus no longer binding. We then solve the problem with each of these $A_{95\%}$ values and observe, in each case, the optimal *fuel allocation* decisions, i.e. the forward-fuels (z_{js}^{MGO-F} and z_{js}^{HFO-F}) and spot-fuels (z_{js}^{MGO-S} and z_{js}^{HFO-S}) consumed for every scenario $s \in S$. The amount of CO_2 emitted (in tonnes) for every scenario s can then be calculated using the following formula:

$$CO_2\ Emitted = \sum_{j \in J} \left[3.082(z_{js}^{MGO-S} + z_{js}^{MGO-F}) + 3.021(z_{js}^{HFO-S} + z_{js}^{HFO-F}) \right] \quad (17)$$

Out of 100 scenarios, we can then find the five scenarios with the highest amounts of CO_2 emitted, and calculate their average as the worst-case CO_2 emission for each given $A_{95\%}$ value.

Table 3: Worst-case CO_2 emissions under different risk aversion levels

Value set for $A_{95\%}$ (maximum CVaR)									
[1000 USD]	388	389	**390***	391	392	393	395	400	Risk-neutral
%	-0.51	-0.26	**0.0**	+0.26	+0.51	+0.77	+1.28	+2.56	-
Worst-case CO_2 emitted (average of five worst scenarios out of 100)									
[tonnes]	5653	5695	**5785**	5787	5890	5930	6046	6046	6046
%	-2.28	-1.56	**0.0**	+0.03	+1.82	+2.51	+4.41	+4.41	+4.41

* Benchmark case with "standard" risk aversion.

Table 3 displays the results comparing the worst-case CO_2 under different risk aversion levels ($A_{95\%}$ values). We may observe that the worst-case CO_2 emissions increase when the company lowers its risk aversion level (or accepts a higher $A_{95\%}$ value). We may also notice that the amount of CO_2 emitted stops increasing and remains at 6046 tonnes when $A_{95\%}$ is above 395,000 USD.

Recall that the stochastics in our model come from the uncertain spot-fuel prices, creating risk on the total bunker costs. The introduction of CVaR constraints is there-

[1] It is feasible and reasonable to restrict the risk level to such extent in this test because the forward-fuel prices are set to be only marginally higher than the expected spot-fuel prices.

fore to contain such risk in the extreme cases. When the risk attitude is more relaxed in a shipping company's bunker risk management, i.e. with higher $A_{95\%}$, the company will have a higher willingness to take risks and rely more on the fuels from the spot market, rather than buying from the forward market. This actually allows the shipping company to operate the ship with higher flexibility in terms of more freedom to apply ECA-evasion and/or speed differentiation strategies, in order to avoid consuming the more expensive MGO. In contrast, for example, if a fair amount of MGO is already hedged, the shipping company's routing decisions may be restricted to the more traditional "shortest but more ECA involved" alternative, just to commit to the hedging contract and thus avoid paying too much penalty for unused MGO eventually. In Table 4, we show the fuel consumption for a specific scenario (where the spot prices for MGO and HFO are 413 USD/tonne and 140 USD/tonne, respectively) under different risk aversion levels. We can see that the total fuel consumption (bottom row in Table 4) increases when setting a higher $A_{95\%}$, and hence the CO_2 emissions also increase (since the emission factors for MGO and HFO are practically the same). This is due to the fact that when relying more on spot fuels (at higher $A_{95\%}$) and in the light of the significant price difference between MGO and HFO, the ship is sailing more "aggressively": such as evading ECA at much as possible and sailing as slowly as possible inside ECA (see Appendix 1 for details). The aggressive sailing has brought down the consumption of MGO but increased HFO consumption even more, which is beneficial in terms of total bunker costs but leads to an increase in total fuel consumption and eventually more CO_2 emitted. Once the $A_{95\%}$ exceeds 395,000 USD, nevertheless, the pattern of fuel consumption for both fuels and thus the sailing behavior remain stable in the worst scenarios, since the sailing behavior in these scenarios has already been pushed to the most aggressive level. Therefore, the average CO_2 emissions in the worst scenarios remain unchanged after the $A_{95\%}$ surpasses 395,000 USD, as observed in Table 3.

Table 4: Example of fuel consumption for a particular scenario under different risk aversion levels

Value set for $A_{95\%}$ (1000 USD)	388	389	390	391	392	393	$\geq 395^*$
MGO consumption (tonnes)	482.2	473.1	455.4	454.4	435.5	426.5	404.8
HFO consumption (tonnes)	1379.4	1402.6	1449.8	1451.9	1504.5	1527.8	1588.5
Total consumption (tonnes)	1861.6	1875.7	1905.2	1906.3	1940.0	1954.2	1993.3

* Including the risk-neutral case.

It is important to notice that the above results are based on studying the *worst-case* CO_2 emissions under different risk aversion levels, which show a clear ten-

dency that the imposition of financial risk control measures (CVaR constraints) is also, to a certain degree, able to contain the "environmental risk" (CO_2 emissions in the worst scenarios). On the other hand, the relationship between *average* CO_2 emissions and risk aversion level is more complicated, and is influenced by how much more expensive MGO is than HFO.

4.1.2 Influence of price gap between MGO and HFO

In our model, the base prices for MGO and HFO (see Sec. 3.2), 375 USD/tonne and 150 USD/tonne, respectively, refer to the spot prices observed in Dec 2015, and are used as expected spot prices for the planning period. This has lead to an Expected Spot Price Gap (ESPG in short) of 225 USD/tonne. In the following test, we aim to study how *average* CO_2 emissions change with different ESPG. This is done by altering the base price for MGO and hence the ESPG, solving the corresponding MBM problem, and observing the average amount of CO_2 emitted across all scenarios (instead of the 5-worst scenarios). We also test for two risk settings: standard risk-averse (see Sec. 4.1.1) and risk-neutral.

Table 5: Average CO_2 emissions at different ESPG, for both standard risk-averse & risk-neutral settings.

ESPG (USD/tonne)	100	150	200	250	260	270	300	350	400
CO_2 (tonnes) Risk-averse	5586.7	5618.2	5655.6	5743.3	5852.3	5988.1	6023.1	6045.2	6046.4
CO_2 (tonnes) Risk-neutral	5561.0	5619.7	5670.7	5821.2	5869.0	5913.0	5999.2	6043.8	6046.4
Difference%*	-0.46	+0.03	+0.27	+1.36	+0.29	-1.25	-0.40	-0.02	0.00

* Relative increase in CO_2 for the Risk-neutral case compared to the Risk-averse case.

Table 5 displays the average amounts of CO_2 emitted, for both standard risk-averse and risk-neutral settings, at various ESPG ranging from 100 USD/tonne to 400 USD/tonne. The corresponding expected spot MGO ranges from 250 to 550 USD/tonne while the expected spot HFO is fixed at 150 USD/tonne. We can clearly see from Table 5 that for the risk-averse setting, the amount of CO_2 emitted becomes higher with increasing ESPG. It is also the case for the risk-neutral setting. This is in fact consistent with the conclusion shown in Fagerholt et al. (2015), that is, in general, CO_2 emissions would also increase when the price gap between MGO and HFO increases, due to a higher tendency to implement ECA-evasion and speed differentiation strategies. However, when comparing the CO_2 emissions between risk-averse and risk-neutral settings, i.e. the **Difference%** row of Table 5, we cannot easily tell which risk attitude is more "environmentally friendly". We further illus-

trate in Fig. 7 the comparison of average CO_2 between risk-averse and risk-neutral settings.

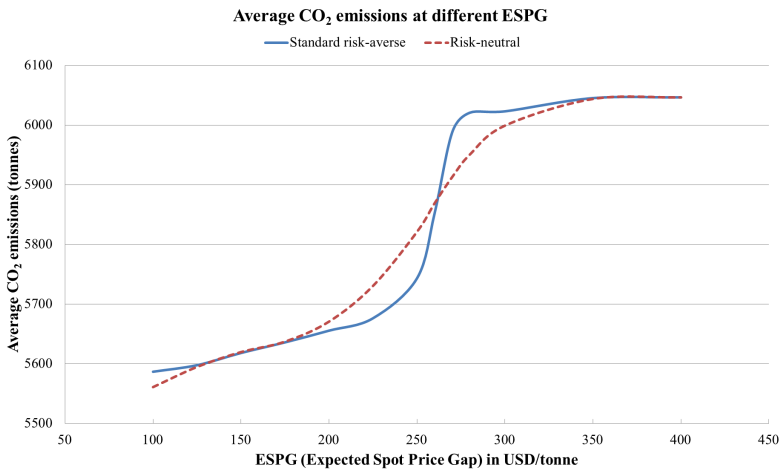

Fig. 7: Difference of expected CO_2 emissions between risk-averse and risk-neutral cases under different levels of price gap

In Fig. 7, the average CO_2 emitted at different ESPG under the standard risk-averse setting is represented by the solid line, and the risk-neutral setting by the dashed line. Unlike the results shown in Sec. 4.1.1, where stronger risk aversion leads to a lower worst-case CO_2 emissions (which is, in fact, a general trend regardless of ESPG according to our experiments), the effect of risk aversion on average CO_2 emissions is undetermined, and depends upon the specific ESPG that we face. For example, in Fig. 7, when the ESPG is around 250 USD/tonne, the risk-averse setting has lower average CO_2 emissions than the risk-neutral case; whereas at around 270 USD/tonne the opposite situation is observed.

In order to explain this somewhat surprising result, we first need to explain what we call a *jump* in sailing behavior. If there is no price gap between MGO and HFO, the shipping company has no incentive to change its sailing behavior, and thus sails the traditional leg option (shortest path) between two ports in the same ECA. When the price gap increases, a leg option change will not immediately occur. The vessel will stick to the shortest path until the price gap between MGO and HFO reaches a certain level, and then switch to another leg option, looking something like Leg Option 2 in Fig. 5; the sailing pattern makes a *jump*. Fig. 8 is used to illustrate the principle of a jump. The solid line represents the traditional leg option between two ports located inside the same ECA, the dash-dot line illustrates the leg option following a jump. For simplicity of the argument, let us simply assume that one universal speed is applied both in- and outside ECA. Hence, fuel consumption is proportional to distance. The fuel cost for the traditional leg is $P^{MGO} \times a$ while the

total bunker cost for the "Jump-to" leg option is $P^{MGO} \times 2d + P^{HFO} \times (a-2c)$. Hence, until the MGO price becomes $\frac{a-2c}{a-2d}$ times as high as the HFO price, it is cheaper to sail the shortest path and a jump will not be triggered. However, once the price gap exceeds that level, the optimal leg option switches to the "Jump-to" leg option and the jump occurs. Note that jumps are a natural part of the underlying problem and not caused by the fact that we have discretized sailing patterns into possible leg options. Furthermore, if time and speed considerations are involved, the "Jump-to" leg option will need a higher average speed, thus higher fuel consumption to maintain the schedule, which leads to a even higher price gap to trigger the jump.

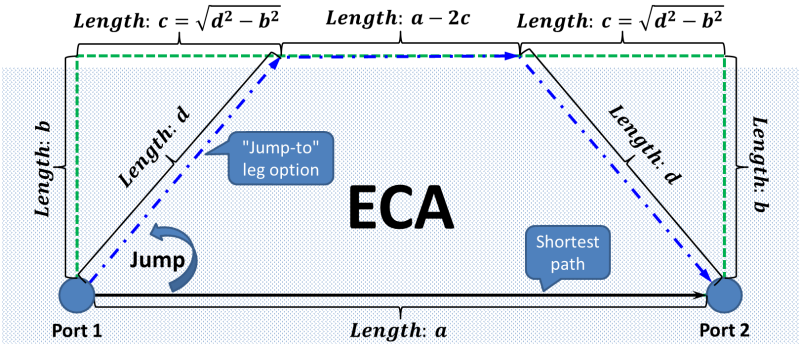

Fig. 8: Simple example illustrating a jump in sailing behavior change

A risk-averse company relies mainly on the forward market while using small amounts of spot-fuels as supplements. Moreover, the forward price difference approximately equals the ESPG since the prices of the forward fuels are set to be just marginally higher than the expected spot fuel prices (basis prices). Therefore, the actual price gap which decides the sailing behavior in the risk-averse setting is significantly affected by the ESPG, and only slightly influenced by the Realized Spot Price Gap (RSPG in short) in each scenario. The RSPG in Scenario s can be expressed as:

$$RSPG_s = ESPG + (I_s^{MGO} - I_s^{HFO}) \tag{18}$$

where I_s^{MGO} and I_s^{HFO} represent the price increments of MGO and HFO, respectively, in Scenario s. The risk-neutral company, however, is more willing to take market risks and thus only buys from the spot market. Hence, in the risk neutral case, the sailing pattern in each specific scenario purely depends on the RSPG in that scenario. In sum, the price gaps in most scenarios in the risk-averse setting are approximately the same as the ESPG while the price gaps in the risk-neutral setting (RSPG) differ substantially from scenario to scenario.

Since most scenarios in the risk-averse setting have similar price gaps, the jump happens almost simultaneously in these scenarios when the ESPG increases to the

level that satisfies the requirement illustrated in Fig. 8. Such a clustered change in sailing behavior (thus CO_2 emissions) in most scenarios brings a sudden and major increase in average CO_2 emissions in the risk-averse setting, as observed in Fig. 7. From Eq. 18, we see that RSPG increases together with the ESPG, but such that the scenario with the largest price increment difference will also have the largest RSPG. Hence, when ESPG increases, these scenarios with large price increment differences will first trigger a jump. Then the scenarios with moderate price increment differences (thus moderate RSPGs) follow along with the increase of ESPG, and finally the jump occurs in the scenarios which have small price increment differences (thus small RSPGs). As we can see, contrary to the clustered jump in the risk-averse setting, the jump in the risk-neutral setting happens gradually from the scenarios with larger RSPGs to the ones with smaller RSPGs. The corresponding effect on average CO_2 emissions is much more widely distributed along the ESPG axis, which eventually leads to a smoother increasing curve for the risk-neutral setting, as witnessed in Fig. 7.

To summarize, in this section we show that the shipping company's risk attitude has impact on its CO_2 emissions in various ways. On one hand, the worst-case CO_2 emissions will be reduced by financial risk control measures, i.e. a stronger risk aversion will lead to less CO_2 emitted in the worst scenarios; on the other hand, the effect of risk aversion on average CO_2 emissions is undetermined, and is influenced by the expected price gap between MGO and HFO on the spot market.

4.2 Impact of hedging strategies on CO_2 emissions

We now study how different hedging strategies affect a shipping company's expected CO_2 emissions. For all experiments presented in this section, we assume the company's risk attitude is always standard risk-averse (see Sec. 4.1.1), and the expected CO_2 emissions refer to the average amount of CO_2 emitted across all scenarios.

Using the input data given in Sect. 3, we can first obtain the optimal hedging amounts of both MGO and HFO by solving the stochastic MBM problem to optimality. We then fix the hedging decision for one fuel, HFO for instance, and change the hedging amount of the other (MGO) to get different combinations of hedging decisions. For each such combination, we solve the problem after fixing the hedging decisions accordingly, and record the expected CO_2 emissions. The results are shown in Fig. 9a, where the hedged MGO varies from 70% to 120% of its optimal amount. We also show in Fig. 9b the opposite case in which we vary the hedging amount for HFO while fixing the hedged MGO at its optimal amount.

From the two charts in Fig. 9 we can see that the expected CO_2 emissions will (a) decrease when hedging more MGO, and (b) increase when hedging more HFO. These changes in CO_2 emissions may be explained by the changes in the company's willingness to apply ECA-evasion and speed differentiation strategies. As mentioned earlier, when more MGO is hedged, in order to commit to the forward

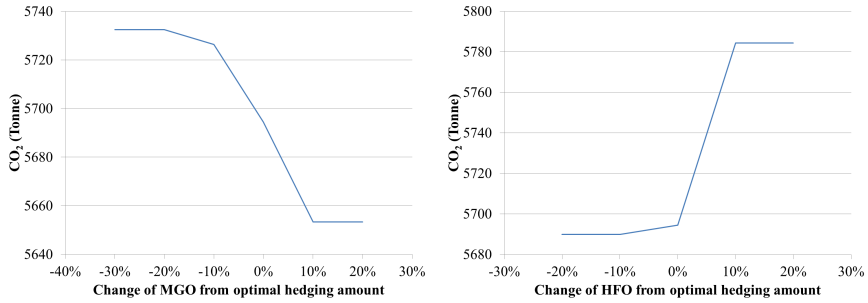

(a) CO_2 under different MGO hedging amount (b) CO_2 under different HFO hedging amount

Fig. 9: Expected CO_2 emissions under different fuel hedging strategies

contract and avoid paying too much penalty for unused forward MGO, the company may be restricted to the traditional "shorter but more ECA involved" routes. In this case, the *total* fuel consumption (MGO&HFO) is usually lower because of the shorter total distance sailed, hence the CO_2 emissions are also lower. On the other hand, when more HFO is hedged, the company may be more likely to sail "aggressively", e.g. with as little ECA involvement as possible, in order to consume more HFO. As a result, the total sailing distance is usually longer, which eventually leads to higher total fuel consumption and more CO_2 emitted.

Note that the above tests only show how expected CO_2 emissions change when altering the hedging amount of one type of fuel alone. In addition, apart from the environmental impact, different hedging decisions may also affect the total bunker costs, which is more of a concern for most shipping companies. Therefore in the following tests, we demonstrate the effects of simultaneously changing the hedging amounts of MGO and HFO, both environmentally (in terms of expected CO_2 emissions) and financially (in terms of expected total bunker costs and worst-case total bunker costs). We seek to provide an insight into the question: can we effectively reduce CO_2 emissions through different hedging strategies? And at what cost?

Let us look at two 3-D charts in Fig. 10. In both charts, we use the changes (%) in the hedging amounts of MGO and HFO (relative to their respective optimal amounts) as x- and y- axes, respectively. For Fig. 10a, we show two plotted surfaces representing expected CO_2 emissions (bottom surface) and expected total bunker costs (top surface), both are changes (%) relative to their corresponding values obtained with the optimal hedging decisions. For Fig. 10b, the surface of expected CO_2 emissions remains the same, and we also show the surface for the worst-case total bunker costs, computed as the average of the five worst scenarios out of 100. Let us further focus on the red areas in the two charts, where the x- (change in MGO) values and y- (change in HFO) values correspond to [+5%,+10%] and [-6%,-2%], respectively. Therefore, by hedging 5% to 10% more on MGO and 2% to 6% less on HFO, we are able to reduce expected CO_2 emissions by 0.75% to 1.63%. This is achieved at the expense of increasing the expected total bunker costs by 0.04%

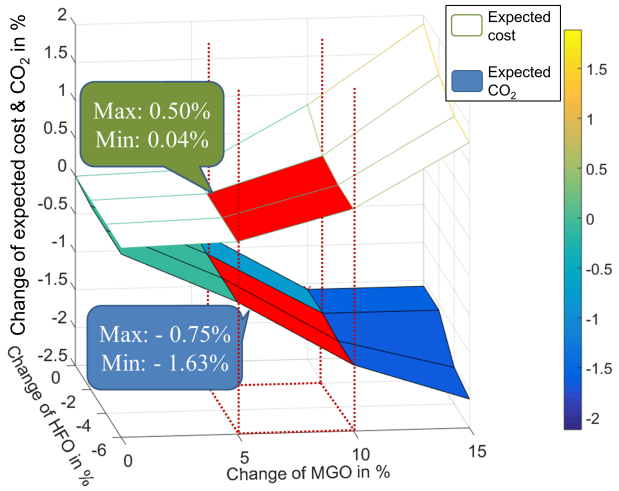

(a) Surfaces for Expected Total Bunker Costs & Expected CO_2 emissions

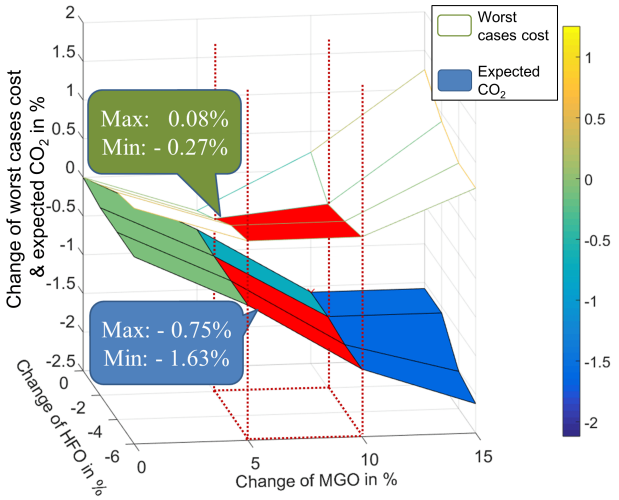

(b) Surfaces for Worst-case Total Bunker Costs & Expected CO_2 emissions

Fig. 10: Illustration of the relation between CO_2 emissions and expected & worst-case total bunker costs under different hedging strategies.

to 0.50%, which are not significant. Furthermore, we show in Fig. 10b that such reduction in CO_2 sometimes even coincides with an improved situation (decrease) in the worst-case bunker cost (ranging from -0.27% to 0.08%). These results are meant to provide an example that sometimes a shipping company can achieve noticeable reduction in CO_2 emissions with little sacrifice on its financial costs by changing the

hedging strategies. For any single player in maritime transportation, such reduction may not be significant. But for the shipping industry on a global scale, this could become a sizable contribution if more companies are coming to the realization of the potential environmental benefits of proper design of hedging and other bunker risk management measures.

5 Conclusion

Bunker risk management is widely practiced in the shipping industry to reduce financial risk and can be vital for a shipping company to remain competitive. Nevertheless, dramatic changes have taken place after the introduction of the ECA regulation. In this paper, we use a stochastic Maritime Bunker Management (MBM) model and a case study on a major liner shipping company to show that bunker risk management has impacts on the company's CO_2 emissions.

We first study the impact of the shipping company's risk attitude on its CO_2 emissions. The results show that stronger risk aversion can also lead to lower "environmental risk", i.e. less CO_2 emissions in the worst cases. Meanwhile, we also show that the effect of risk aversion on average CO_2 emissions is undetermined, and is influenced by the expected price gap between MGO and HFO on the spot market. We then study the impact of hedging strategies on CO_2 emissions. We show that a shipping company can sometimes achieve noticeable reduction in CO_2 emissions with little sacrifice on its financial costs by changing its hedging strategies.

Acknowledgements

The authors acknowledge financial support from the project "Green shipping under uncertainty (GREENSHIPRISK)" partly funded by the Research Council of Norway under grant number 233985.

References

Alizadeh, A. H., Kavussanos, M. G., and Menachof, D. A. (2004). Hedging against bunker price fluctuations using petroleum futures contracts: constant versus time-varying hedge ratios. *Applied Economics*, 36(12):1337–1353.

Andersson, H., Fagerholt, K., and Hobbesland, K. (2015). Integrated maritime fleet deployment and speed optimization: case study from RoRo shipping. *Computers & Operations Research*, 55:233–240.

Cames, M., Graichen, J., Siemons, A., and Cook, V. (2015). Emission reduction targets for international aviation and shipping. http:

//www.europarl.europa.eu/thinktank/en/document.html?reference=IPOL_STU(2015)569964. (accessed 25.06.2016).

Cariou, P. (2011). Is slow steaming a sustainable means of reducing co_2 emissions from container shipping? *Transportation Research Part D*, 16(3):260–264.

Clarkson (2015). Clarkson Research Services website. https://sin.clarksons.net/. (accessed 11.01.2016).

Corbett, J. J., Wang, H., and Winebrake, J. J. (2009). The effectiveness and costs of speed reductions on emissions from international shipping. *Transportation Research Part D*, 14(8):593–598.

De, A., Mamanduru, V. K. R., Gunasekaran, A., Subramanian, N., and Tiwari, M. K. (2016). Composite particle algorithm for sustainable integrated dynamic ship routing and scheduling optimization. *Computers & Industrial Engineering*, 96:201–215.

Doudnikoff, M. and Lacoste, R. (2014). Effect of a speed reduction of containerships in response to higher energy costs in sulphur emission control areas. *Transportation Research Part D*, 28:51–61.

Fagerholt, K., Gausel, N. T., Rakke, J. G., and Psaraftis, H. N. (2015). Maritime routing and speed optimization with emission control areas. *Transportation Research Part C*, 52:57–73.

Gencer, M. and Unal, G. (2012). Crude oil price modelling with Lévy process. *International Journal of Economics and Finance Studies*, 4(2):139–148.

Gu, Y., Wallace, S. W., and Wang, X. (2016). Integrated maritime bunker management with stochastic fuel prices and new emission regulations. Working Paper 13/16, Department of Business and Management Science, Norwegian School of Economics.

Høyland, K., Kaut, M., and Wallace, S. W. (2003). A heuristic for moment-matching scenario generation. *Computational optimization and applications*, 24(2):169–185.

ICS (2015). International Chamber of Shipping website. http://www.ics-shipping.org/shipping-facts/shipping-and-world-trade. (accessed 05.02.2016).

Kaut, M. and Wallace, S. W. (2007). Evaluation of scenario-generation methods for stochastic programming. *Pacific Journal of Optimization*, 3(2):257–271.

Kontovas, C. A. (2014). The green ship routing and scheduling problem (gsrsp): A conceptual approach. *Transportation Research Part D*, 31:61–69.

Krichene, N. (2008). Crude oil prices: Trends and forecast. Working Paper WP/08/133, International Monetary Fund.

Lindstad, H., Asbjørnslett, B. E., and Strømman, A. H. (2011). Reductions in greenhouse gas emissions and cost by shipping at lower speeds. *Energy Policy*, 39(6):3456–3464.

Maloni, M., Paul, J. A., and Gligor, D. M. (2013). Slow steaming impacts on ocean carriers and shippers. *Maritime Economics & Logistics*, 15(2):157–171.

Menachof, D. A. and Dicer, G. N. (2001). Risk management methods for the liner shipping industry: the case of the bunker adjustment factor. *Maritime Policy & Management*, 28(2):141–155.

Norstad, I., Fagerholt, K., and Laporte, G. (2011). Tramp ship routing and scheduling with speed optimization. *Transportation Research Part C*, 19(5):853–865.

Pedrielli, G., Lee, L. H., and Ng, S. H. (2015). Optimal bunkering contract in a buyer-seller supply chain under price and consumption uncertainty. *Transportation Research Part E*, 77:77–94.

Psaraftis, H. N. and Kontovas, C. A. (2009). CO_2 emission statistics for the world commercial fleet. *WMU Journal of Maritime Affairs*, 8(1):1–25.

Qi, X. and Song, D.-P. (2012). Minimizing fuel emissions by optimizing vessel schedules in liner shipping with uncertain port times. *Transportation Research Part E*, 18(4):26–31.

Tai, H.-H. and Lin, D.-Y. (2013). Comparing the unit emissions of daily frequency and slow steaming strategies on trunk route deployment in international container shipping. *Transportation Research Part D*, 21:26–31.

Wang, X. and Teo, C. C. (2013). Integrated hedging and network planning for container shipping's bunker fuel management. *Maritime Economics & Logistics*, 15(2):172–196.

Wong, E. Y., Tai, A. H., Lau, H. Y., and Raman, M. (2015). An utility-based decision support sustainability model in slow steaming maritime operations. *Transportation Research Part E*, 78:57–69.

Appendix 1

The detailed speed-routing decisions in scenario No. 26 under different maximum CVaR values are shown in the following table.

Table 6: Sailing behaviors in scenario No. 26 under different risk aversions

Max CVaR (1000 USD)	388	389	390	391	392	393	Neutral
Leg 1							
Leg Option	4	*5*	*5*	*5*	*5*	*5*	*5*
ECA/non-ECA distance (nautical mile)	496/905	*408/1062*	*408/1062*	*408/1062*	*408/1062*	*408/1062*	*408/1062*
ECA/non-ECA speed (knot)	15/15	15/15	15/15	15/15	15/15	15/15	15/15
Leg 2							
Leg Option	3	3	*5*	*5*	*5*	*5*	*5*
ECA/non-ECA distance (nautical mile)	524/906	524/906	*397/1241*	*397/1241*	*397/1241*	*397/1241*	*397/1241*
ECA/non-ECA speed (knot)	15/15	15/15	15/15	15/15	15/15	15/15	15/15
Leg 3							
Leg Option	1	1	1	1	*4*	*4*	*4*
ECA/non-ECA distance (nautical mile)	632/0	632/0	632/0	632/0	*443/515*	*443/515*	*443/515*
ECA/non-ECA speed (knot)	15/15	15/15	15/15	15/15	15/15	15/15	15/15
Leg 4							
Leg Option	4	4	4	4	4	4	*5*
ECA/non-ECA distance (nautical mile)	889/2652	889/2652	889/2652	889/2652	889/2652	889/2652	*752/2903*
ECA/non-ECA speed (knot)	15/20.6	15/20.6	*15/20.1*	*15/20.1*	*15/20.1*	*15/20.1*	*15/20.5*
Leg 5							
Leg Option	5	5	5	5	5	5	5
ECA/non-ECA distance (nautical mile)	751/3428	751/3428	751/3428	751/3428	751/3428	751/3428	751/3428
ECA/non-ECA speed (knot)	15/18.1	15/18.1	15/18.1	15/18.1	15/18.1	15/18.1	15/18.1